

# Effect of Flexible Vegetation on the Force's on Structures Due to Long Waves

Noarayanan.L<sup>\*1</sup>, Murali. K<sup>2</sup>, Sundar.V<sup>3</sup>

<sup>1</sup>Research Fellow, Nanyang Technological University, Division of Environmental & Water Resources Engineering, 639798, Singapore

<sup>2,3</sup>Professor, Department of Ocean Engineering, Indian Institute of Technology Madras, Chennai 600036, India

<sup>\*1</sup>noara\_l@hotmail.com; <sup>2</sup>murali@iitm.ac.in; <sup>3</sup>vsundar@iitm.ac.in

**Abstract-** The wave run-up over beaches and coastal structures is the most important parameter that dictates the fixing of the crest elevation in order to avoid flooding during extreme events, like tsunami, typhoon and storm surge. The choice of type depends on the purpose for which it is proposed. This paper deals with the study of efficiency of vegetation as a buffer system in attenuating the incident ocean waves through a well-controlled experimental program. The focus of this study was on the measurement of forces due to Cnoidal waves on a model building mounted on a slope in the presence of varying densities of vegetation, starting with no vegetation present. In order to obtain a holistic view of the wave-vegetation interaction problem chosen for study, the vegetative parameters like the width of the green belt, its position from the reference line, diameter of the individual stems, and the spacing between them and their rigidity were varied. This paper introduces two new parameters, namely, Vegetation-Flow Parameter that combines the characteristics of vegetation and waves and Vegetal Parameter that describes the width of green belt (BG), spacing (SP) and diameter (D) of the vegetation. The details of experimental test set-up, measurement procedures, and results on the effect of vegetation on the variation of forces on a model building are presented and discussed in this paper.

**Keywords-** Cnoidal Waves; Vegetal Stems; Wave Force; Vegetal Drag; Vegetation Flow Parameter; Staggered Vegetation; Vegetal Parameter

## I. BACKGROUND

During the ingress of the great Indian Ocean tsunami, the vegetation on the seaside of existing structures along the coast has proved to be good attenuators in reducing the inundation heights and distance into the land, the phenomena of which are not well understood. Further, as a part of the mitigation program, one would need the information on the percentage of reduction in the vertical run-up and inundation distance over structures or open beaches due to the presence of vegetation. This prompted the investigators to carry out a detailed experimental study.

Hiraishi and Harada (2003) carried out tests in a tsunami channel to investigate the efficiency of a chemical porous medium representing a greenbelt barrier, in reducing the run-up and inundation distance. It was claimed that the greenbelt had a similar efficiency in reducing the incident energy as that of coastal dikes composed of wave energy dissipating blocks. Further, the effectiveness of a greenbelt or vegetation was carried out by adopting the 1998 Papua New Guinea tsunami data, through a numerical simulation with a nonlinear long wave model that included the drag

force term. The study concluded that the maximum tsunami run-up height on shore was smaller in presence of a greenbelt. Struve *et al.* (2003) showed that the drag coefficient increases with an increase in the tree surface. A survey along 18 coastal hamlets along the southeast coast of India after the 26 Dec 2004 Indian Ocean tsunami, carried out by Kathiresan and Rajendran (2005) has revealed a significant reduction in tsunami height and inundation of coastal area due to the presence of mangroves and other plantations. Following a detailed study, the plant species that need to be planted along the coast as a mitigation measure were identified. The results of a field survey on the effects of the above tsunami along the coast of Thailand as well as on the aspects of the role of vegetation or greenbelt have been discussed by Hiraishi (2005). The study also emphasized the applicability of greenbelt as a solution for tsunami through a numerical model, according to the model mentioned in the previous line, the eroded volume at a beach with some vegetation was found to be smaller than at a beach with no vegetation. Furthermore, stabilization of sandy beaches was also pointed out as another positive impact of a greenbelt for tsunami disaster mitigation. Kongko (2005) reported an overview on the effectiveness of mangroves and coastal forest in reducing tsunamis along with evidence for its effectiveness against tsunamis. Harada and Imamura (2005) quantitatively evaluated the hydrodynamic effects and damage-prevention functions of coastal forests against tsunamis with a view to using them as tsunami counter measures. They reported that an increase in forest width can reduce not only inundation depth, but also the currents and hydraulic forces behind the coastal forest. Two different coastal species, *Pandanus odoratissimus* and *Cocos nucifera*, which are dominant in Sri Lanka were analyzed by Nandasena and Tanaka (2007) through numerical studies to understand the hydrodynamic behaviour of these species in the case of propagation of a tsunami.

The effects of coastal vegetation on tsunami damage based on field observations were studied by Tanaka *et al.* (2007) after the Indian Ocean tsunami on December 26, 2004 along the southern coast of Srilanka. Sundar *et al.* (2007) conducted a study along the coast of Tamil-nadu (South east coast of India) and Andaman and Nicobar Islands. The study covered the effect of vegetation on the inundation distance and heights due to the great Indian Ocean tsunami of 2004. Having realized the importance of the plantation or bio-shields as one of the most effective

eco-friendly coastal protection measures, there has been a continuous effort by researchers worldwide in understanding the wave vegetation interaction phenomena.

Borrero *et al.* (2006) used the model MOST (method of splitting tsunami), one of only two fully validated hydrodynamic models for operational tsunami propagation and inundation. MOST uses the final dislocation field from the seismic deformation model to initialize hydrodynamic computations. MOST has also accounted the on land crustal deformation from the earthquake and computes the wave evolution and run-up onto dry land over the newly deformed bathymetry and topography. The studies of Danielsen *et al.* (2005) revealed that three of five villages sheltered by mangroves on the seaside experienced no damage, while, the rest two unprotected experienced severe damage due to the propagation of tsunami. Laso-Bayas *et al.* (2011) addressed the influence of coastal vegetation during 2004 tsunami, considering topographical changes and emphasized the need for more dense agro forests in between sea and the coastal communities (i.e., cacao, rubber and multilayered home gardens) as a preparedness for an extreme natural coastal hazard.

Noarayanan *et al.* (2012) conducted a comprehensive laboratory study on the hydraulic resistance characteristics due to a group of slender cylindrical members representing flexible plantation and proposed a new empirical equation for evaluating the Manning's  $n$  friction coefficient for partially submerged flow when, the depth of flow is greater than 0.8 times the undeflected plant height. Noarayanan *et al.* (2012) studied the behaviour of the vegetation due to regular and cnoidal waves propagating over a plane slope of 1: 30 in the presence and absence of vegetation in attenuating run-up thereby conducting laboratory experiments and presented the variation of dimensionless run-up as a function of wave and vegetal parameters. Noarayanan *et al.* (2011) investigated the dynamic pressures exerted on a vertical wall due to cnoidal waves duly subjecting two types of configurations of the green belt with the individual stems of vegetation fixed in tandem and

staggered arrangement and concluded that the staggered arrangement of plantation is more effective in attenuating the incident waves.

The stiffness of the vegetation is one of the major parameter that governs its effectiveness in reducing the flow intensity during the ingress of a tsunami. The results from the nature of the present model study would permit its application to real world situations as it is neither species nor location specific, but depends only on the characteristics of flow and vegetation. The physical processes in the problem chosen that are predominant are the bending behaviour of the vegetation, wake induced vibrations on the downstream of the green belt, its width, diameter of the individual stems of the green belt, spacing between them. The basic purpose of the design of a green belt is to shelter an existing or a proposed structure during an extreme event by reducing the flow intensity, thereby, preventing excess loads on the structure. This would mean that the distance between the structure and the structure will also be an important parameter to be considered in the design process. To account these processes, rigidity has to be modelled and suitable (spacing between the individual stems,  $SP$ / stem diameter,  $D$ ) ratio is to be identified. As tsunami can be approximately characterized by long waves, like Cnoidal waves, such waves are considered for the present study.

## II. EXPERIMENTAL INVESTIGATIONS

A host of parameters that govern the forces on the structures fronted by vegetation were subjected to Buckingham's Pi theorem and the resulting parameters have been grouped in Table.1. The dimensionless wave force on model building/ structure,  $F^*$  is given as,

$$F^* = \left( \frac{F_{max}}{0.5 * \rho g H^2 B_s} \right) \quad (1)$$

TABLE I NON-DIMENSIONAL PARAMETERS FOR THE PRESENT STUDY

| Parameters  | Wave flume (Model) |
|---|--------------------|
| Keulegan Carpenter number, $KC = [(U_{max} T)/B_s]$                       | 31 to 145          |
| Vegetation Flow parameter, $VFP = [EI(BG/D)]/[\rho H^3 V_{avg}^2 (SP/D)]$ | 0.006 to 2.31      |
| Vegetal parameter = $[(BG*SP)/D^2]$                                       | 94 to 8333         |
| Reduced velocity, $V_r = [V_{avg}/(f_i D_i)]$                             | 11-166             |

To represent properly the hydro-elastic interaction of the vegetal stems with the flow, a suitable material for model stems of the green belt had to be identified to represent coastal vegetation in real world. One of the guiding parameters for this purpose is the Young's modulus,  $E$ , which is a measure of the stiffness of an elastic material and is a quantity used to characterize material property. It is defined as the ratio of the uni-axial stress over the uni-axial

strain in the range of stress in which Hooke's Law holds. In general the common timber would be having a value for  $E$  in the range, 10.05 GPa to 15 GPa. The mangrove's Young's modulus,  $E$  value would be around 20.03 GPa. A reference value of 14 GPa, Gan *et al.* (2001) for the individual stem of the green belt is assumed keeping in mind to cover the wide range of  $E$ , a scale ratio of 1:40, for a flow field similar to a tsunami, has been experimented. In

other words, a material with  $E$  value of about 0.35 GPa to be chosen which is quite scanty.

Instead of modelling Young's modulus,  $E$  and second moment of inertia,  $I$  separately, the rigidity  $EI$  has been modelled as a single parameter. Poly Ethylene which has got an  $E$  value of 3.8 GPa has been chosen for the vegetation model fabrication. As we have modelled the rigidity, the above said variation could be adjusted with the variation in  $I$  of the material. Having chosen the model material, the typical prototype dimensions of vegetal stems were fixed in the range of 100 mm – 400 mm. According to the Froude model law of scaling, the base diameter for the individual stem of the model vegetation falls in the range of 1.65 – 5.5 mm, as the rigidity scale factor is  $[SF]^5$ . The bending action of the vegetal model has been scaled there by adopting the base diameter of the vegetal model as per Froude model law of scaling. The above discussion would clearly points out the importance of modelling the rigidity instead of Young's modulus. Forces also to be properly scaled as per Froude model law so as to have an appropriate hydrodynamic interaction between the flow and the vegetal stems. As per the drag/inertia force regime of Chakrabarti, (1983) the vegetal models corresponding diameters at the top portion has been arrived. The vegetal model used for the experiments with varying diameters at top and base for two model vegetations have been shown in Fig. 1. By providing a small clearance between the base and the section, where the diameter changes from a lower to a higher value, we have made the vegetal models bending behaviour unchanged. The bottom root diameter is only to emphasis and ensures the  $EI$  of the vegetal model.

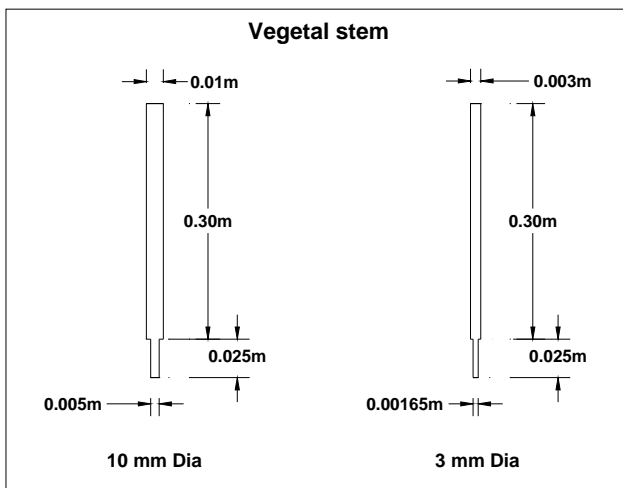


Fig. 1 Typical dimension of vegetal stem

### III. EXPERIMENTAL DETAILS

A wave flume of 72 m in length, 2.0 m wide and 2.7 m deep, situated in Department of Ocean Engineering, Indian Institute of Technology Madras, India has been used for this investigation. The entire width of the flume of 2 m was separated by means of a plywood boards at every 0.66 m, longitudinally. This has been done to handle three different

configurations of tests setups simultaneously. Each of the three separations had a rigid inclined bed with 1 Vertical in 30 Horizontal slope that which would start at a distance of 43.5 m from the end of the wave flume. The inline wave force on the model building/structure kept in the wave flume was measured through a single beam type cantilever component force transducer (HBM). The sensitivity of the load cell considered for the model building/structure of size 0.2 m\*0.2 m and 0.3 m would be around 200 N with an accuracy of 0.1 N. The model building/structure is as shown in Fig. 2.



Fig. 2 Force transducer

The experiments have been carried out in all the three set-ups at the same time. All the tests were carried out by maintaining 1.0 m water depth at the toe of the slope. Green belts of width 0.250 m, 0.625 m and 1.000 m with vegetal stems fixed to the bottom of the slope in a staggered manner were subjected to the wave actions. Two vegetal models with diameters of 10 mm and 3 mm were used to each of the staggered arrangement. Further, two different spacing of 37.5 mm and 75 mm were adopted for each of the two diameters considered. In a nutshell, for the present experiments, two diameters of the vegetation, 2 spacing's of vegetation and 3 width of the green belts resulting in 12 set ups have been considered. A typical configuration of vegetal model with stem diameter,  $D=3$  mm, spacing,  $SP=75$  mm and width of green belt,  $BG=1000$  mm is as shown in Fig. 3 Schematically. For all the combinations mentioned above, tests were carried out to measure the forces for the vegetal parameters on the model structure which represent a building that have been positioned at locations  $G/B$  ratios of 0, 0.5, 1.0 and 1.5. The experiments were done for the cases, viz., (a) structure fronted by vegetal model/ bio shield and (b) structure with no vegetation present. Fig. 4 explains schematically the location of the structure and the green belt/ bio shield adopted for the study. Vegetal parameters,  $D$ ,  $SP$  and  $BG$  adopted for the tests have been mentioned as a block diagram in Fig. 5 along with the values of Vegetal Parameter,  $BG*SP/D^2$ .

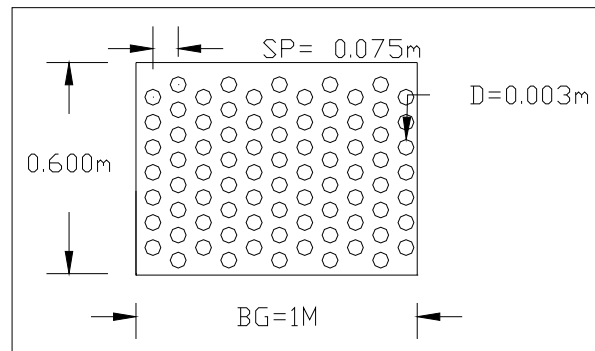


Fig. 3 Schematic diagram of Staggered Configuration of green belt (SP=0.075 m; BG=1 m and D = 0.003 m)

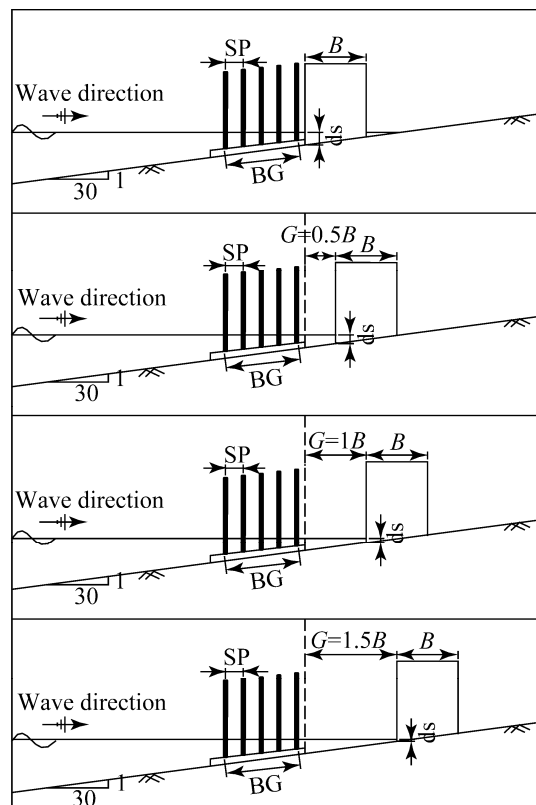


Fig. 4 Definition of variables for Force measurements in the wave flume (Presence of vegetation)

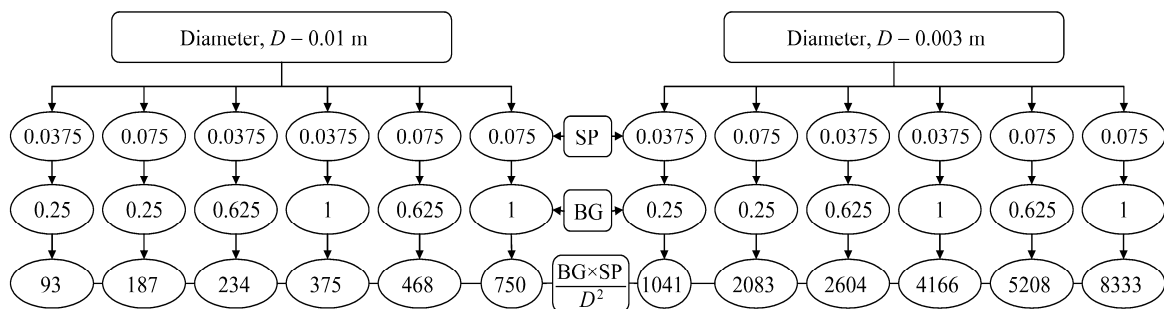


Fig. 5 Block diagram showing the Vegetal Parameter,  $BG \cdot SP / D^2$

An experimental set-up shown in Fig. 6, exhibits the measurement of forces on the structure in presence of

vegetation and with no vegetation present. A 12bit resolution A/D card has been used to capture the signals

from the wave gauges and load cells which are in turn routed through a wave amplifier and recorded for 80 secs duration and stored in a personal computer. The data were

collected at a sampling interval of 0.025 sec. By time domain analysis the peak value of the force,  $F_{max}$  were obtained for the wave and force time histories measured.

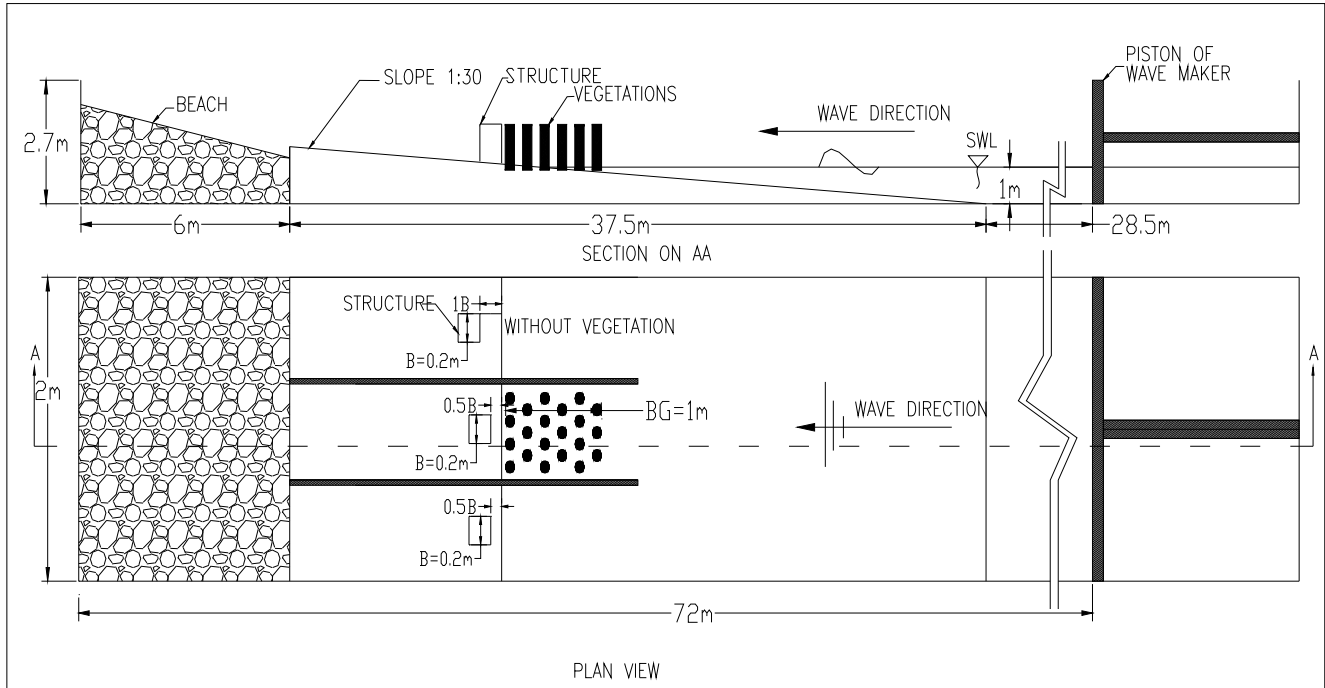


Fig. 6 Experimental set-up for Force measurements in the wave flume for  $G/B=0.5$  and 1

#### IV. RESULTS AND DISCUSSION

The preliminary experiments with the model building/structure which has been rigidly fixed on the sloping bed and housed with a load cell so as to quantify the in-line forces for the case with no vegetation present was subjected to various, Vegetation Flow Parameters. The results obtained were compared with the results of Isaacson (1979) in Fig. 7, which shows a good agreement. This attempt has been done in order to validate the present experimental setup, testing procedures and forces,  $F^*$ . The forces on the model building/structure due to larger Ursell number  $U_r = HL^2/h^3$ , ranging between 18 and 700 (Cnoidal waves) have been measured for the two scenarios, viz., (a) structure fronted by vegetal model/ bio shield and (b) structure with no vegetation present. The forces on the modelled building/structure  $F^* = [(F_{max}) / (0.5 \cdot \rho \cdot g \cdot H^2 \cdot B_s)]$ , has been expressed in a dimensionless form to enable the user to use the model values to the field. Drag and inertia forces for any shaped objects in an oscillating flow field would be quantified by Keulegan-Carpenter,  $KC$  number,  $U_{max} \cdot T/D_s$ , which is a non-dimensional. Wherein,  $U_{max}$  is  $[c = \sqrt{g \cdot h_s (1 + (H/h_s))}]$ , Wiegel (1964) and  $D_s = B_s$  in the current investigation, wherein,  $D_s$  will be the breadth of the structure perpendicular to the wave direction.

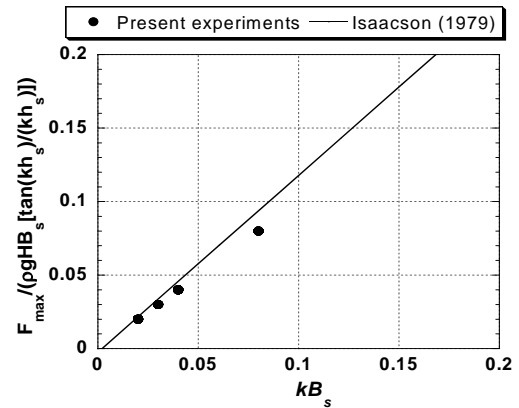


Fig. 7 Comparison of present experimental results with Isaacson (1979)

The variations of  $F^*$  obtained for the tests in presence and absence of vegetation with the vegetation-flow parameter  $VFP$  defined as  $VFP = [EI (BG/D)] / (\rho H^3 V_{avg}^2 (SP/D))$  for the range of  $11 \leq V_r \leq 14$  for  $G/B$  ratios of 0, 0.5, 1, and 1.5 are shown in Fig. 8. The plots corresponding to  $130 \leq V_r \leq 166$  are shown in Fig. 9. From the results it is seen that for the case  $G/B=0$ ; the maximum dimensionless force in the presence of vegetation is found to be about 80 - 95% less than that with vegetation. As the  $VFP$  increases, the force on the structure in the absence of vegetation is found to increase, whereas, this effect is not found to be significant when vegetation is present in front of the structure. For the case of  $G/B=0.5$ , the forces are clearly seen to increase for the structure fronted by vegetation, the rate of increase being higher with an increase in  $VFP$ . For the case of  $G/B = 1$ , although a similar trend in its variation

as observed for  $G/B=0.5$  is seen, the rate of increase in the force is found much lesser. For the last case of  $G/B = 1.5$ , the forces in the presence of vegetation are found to be less compared to that obtained for the earlier two cases. The reason for the above trend in the variation in dimensionless forces is discussed earlier. In addition the kinetic energy of the reformed wave on the lee side of the vegetation may be more in case of  $G/B = 0.5$  while this effect reduces as  $G/B$  increases. Hence most favorable location for the structure is adjacent to the green belt ( $G/B = 0$ ) or away from the green belt by more than  $1.5B$ . The maximum value of the dimensionless force for  $G/B=0, 0.5, 1, 1.5$  is found to be 1.2, 3, 2.6 and 1.3 respectively. Similar behavior observed in the variation of the dimensionless force with the vegetation-flow parameter  $VFP$  for the range of  $130 \leq V_r \leq 166$ .

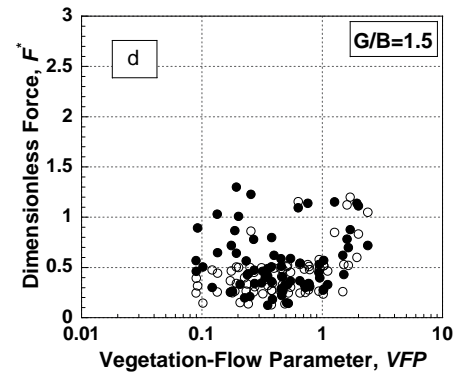
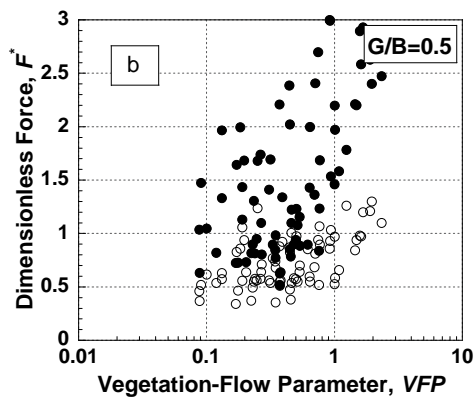
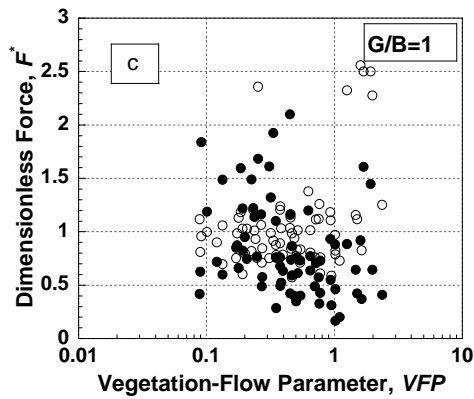
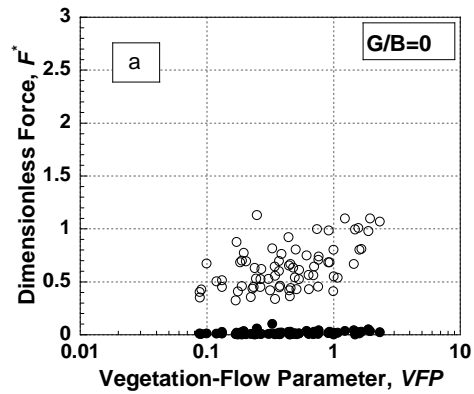
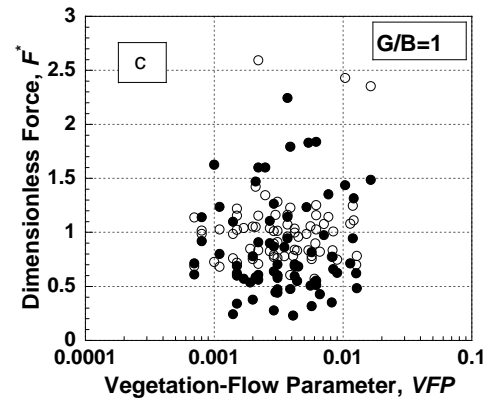
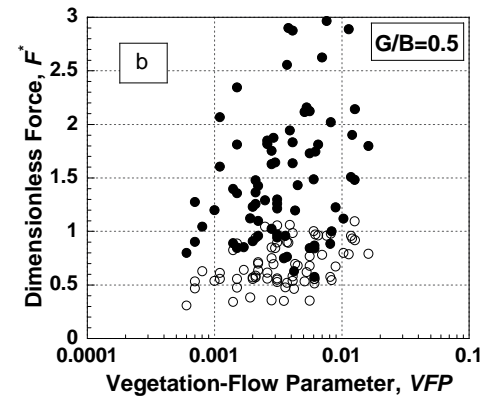
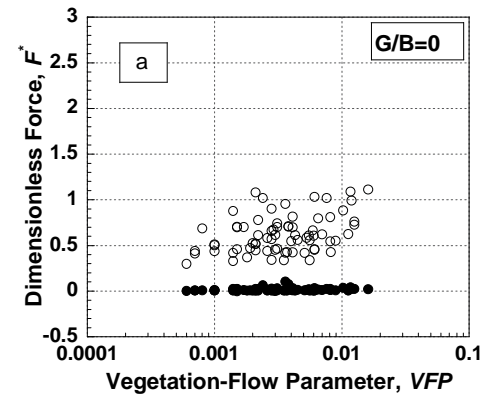


Fig. 8 Variation of Dimensionless Force with Vegetation-Flow Parameter for  $V_r=11$  to 14. (○- No Veg and ● Veg)



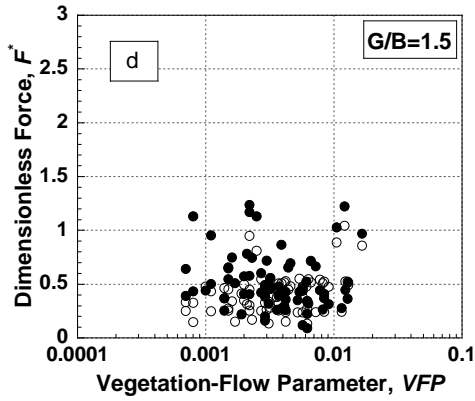


Fig. 9 Variation of Dimensionless Force with Vegetation-Flow

Parameter for  $V_r = 130$  to 166. (○- No Veg and ●-Veg)

It may be noted that a significant scatter exist in the results shown in the above plots. Hence, a new vegetation parameter was introduced for examining the effect of width of green belt  $BG$  and spacing of vegetation  $SP$ . This vegetation parameter is  $[BG*SP/D^2]$ . The advantage of this parameter is that one can examine the combined effects of  $BG$  and  $SP$  that appear in the non-dimensional parameter. Hence, the variations of  $F^*$  with  $VFP$  are again re-plotted for constant  $[BG*SP/D^2]$  and for four different  $G/B$ . The plots corresponding to  $[BG*SP/D^2] = 93$  are projected in Fig. 10. Similar results for a wide spectrum of  $[BG*SP/D^2]$  up to 8333 are shown in Figs. 11 to 21. These results have clearly brought out the effect of  $VFP$  on  $F^*$ . An increasing trend in the  $F^*$  is noticed for all the  $G/B$  for a specific  $[BG*SP/D^2]$ .

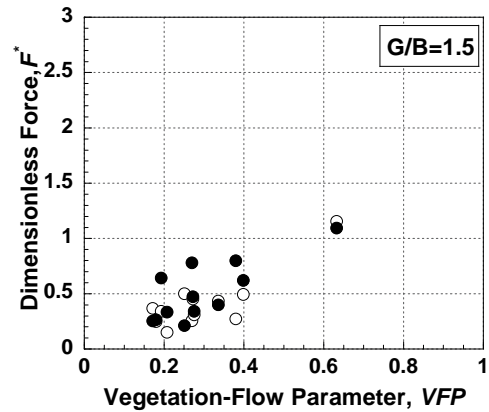
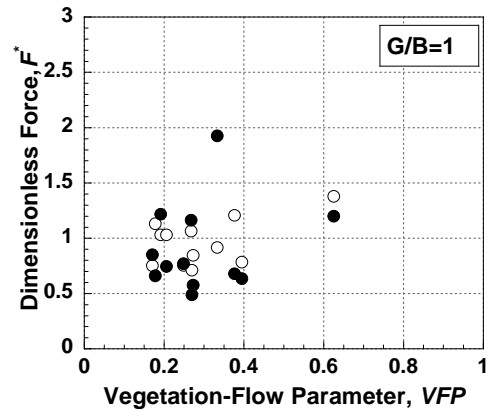
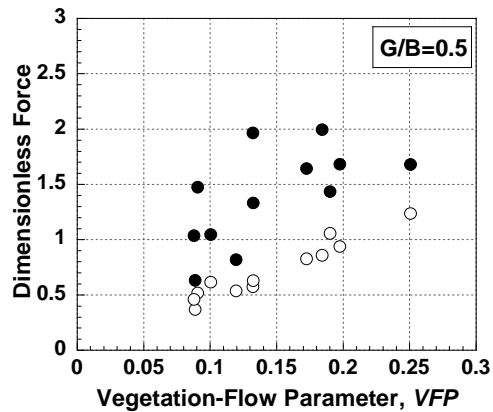
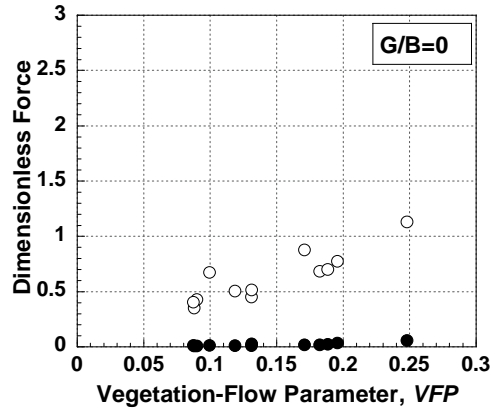
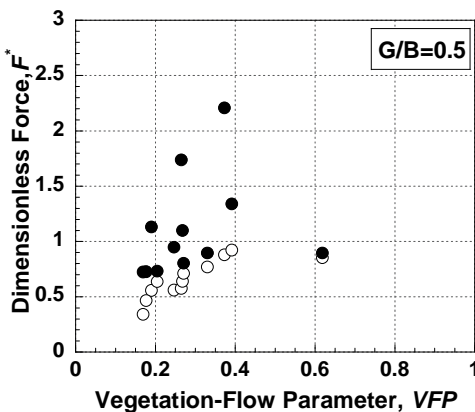
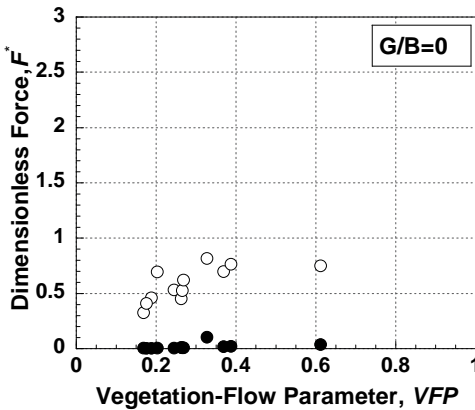


Fig. 10 Variation of Dimensionless Force with Vegetation-Flow

Parameter for  $(BG*SP/D^2) = 93$ . (○-No Veg and ●-Veg)



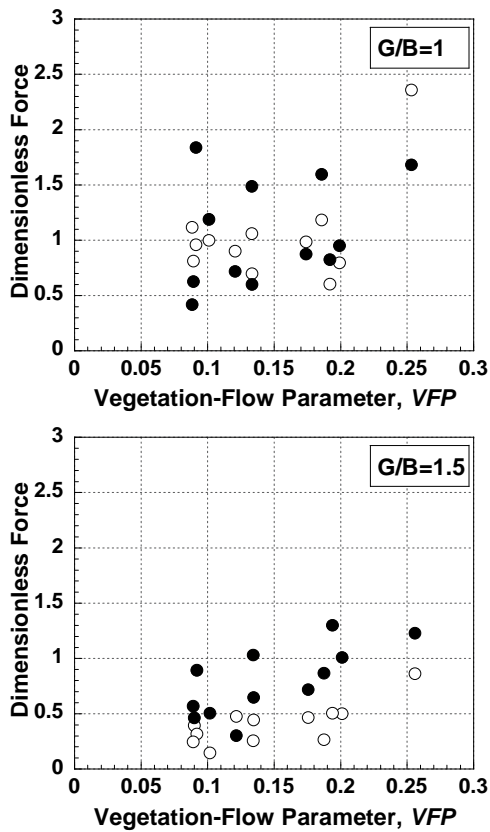


Fig. 11 Variation of Dimensionless Force with Vegetation-Flow Parameter for  $(BG*SP/D^2) = 187$ . (○-No Veg and ●-Veg)

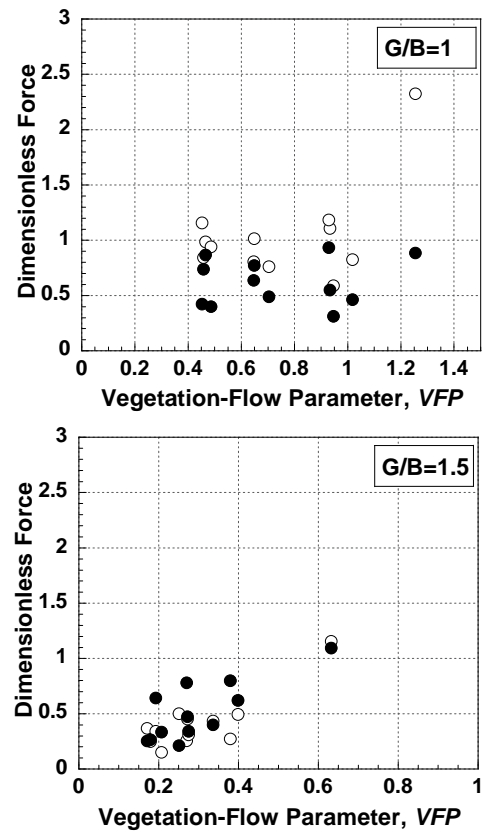
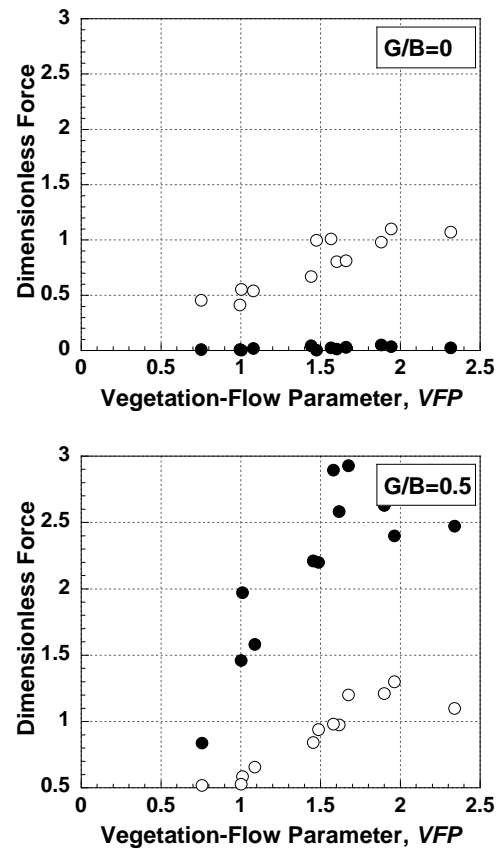
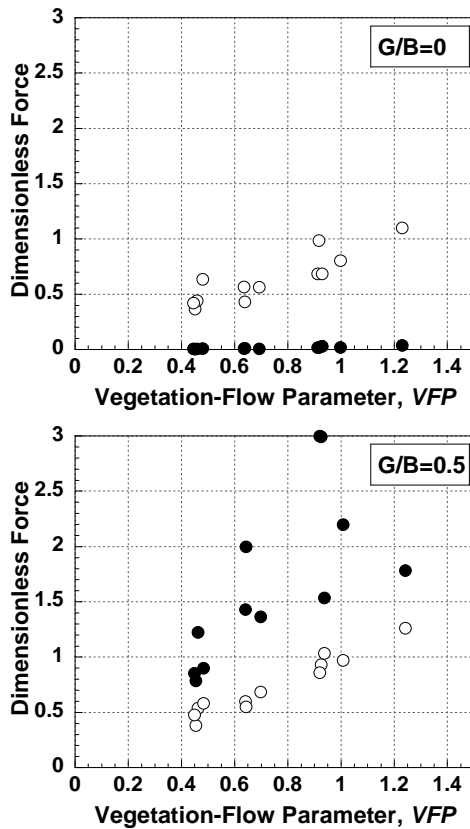


Fig. 12 Variation of Dimensionless Force with Vegetation-Flow Parameter for  $(BG*SP/D^2) = 234$ . (○-No Veg and ●-Veg)





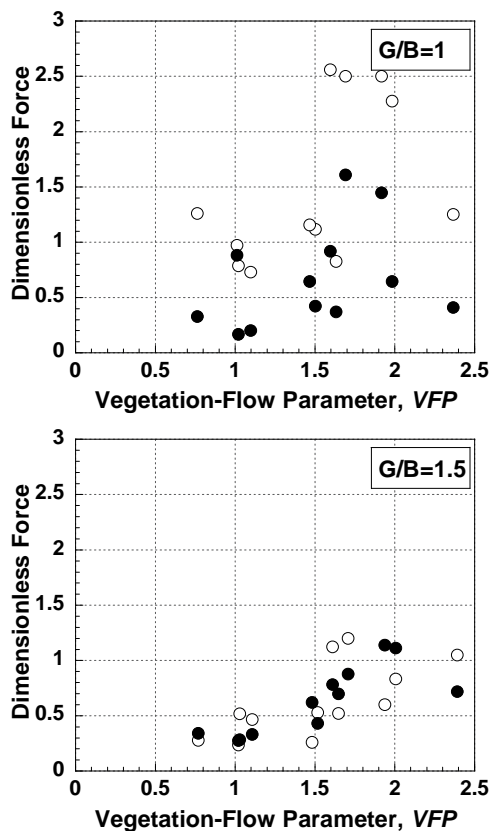


Fig. 13 Variation of Dimensionless Force with Vegetation-Flow Parameter for  $(BG*SP/D^2) = 375$ . (○-No Veg and ●-Veg)

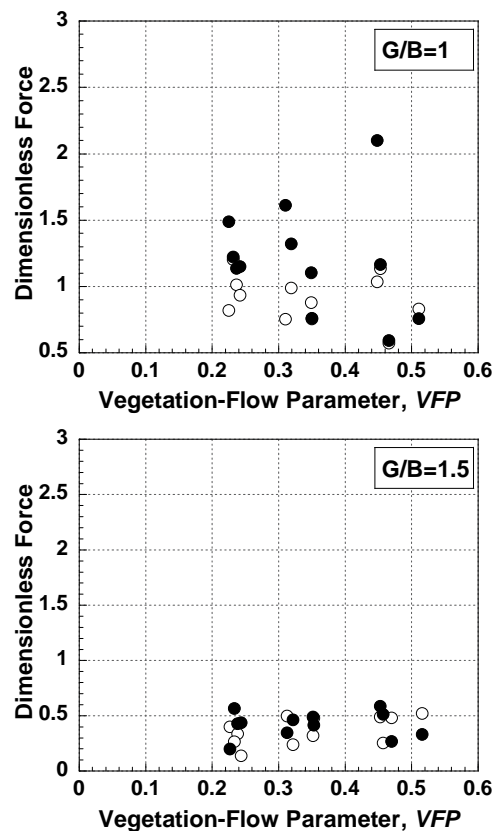
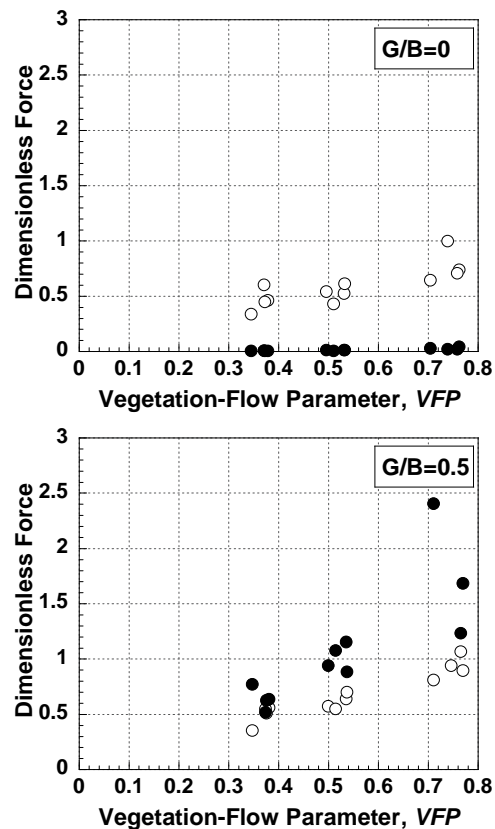
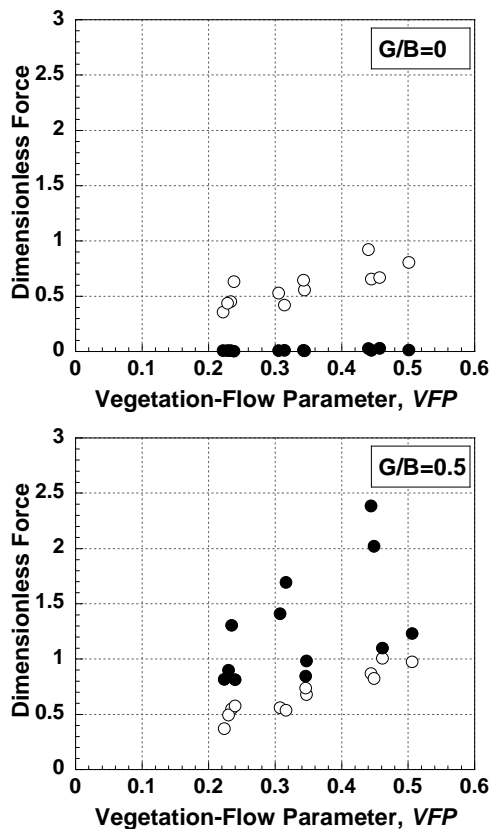


Fig. 14 Variation of Dimensionless Force with Vegetation-Flow Parameter for  $(BG*SP/D^2) = 468$ . (○-No Veg and ●-Veg)



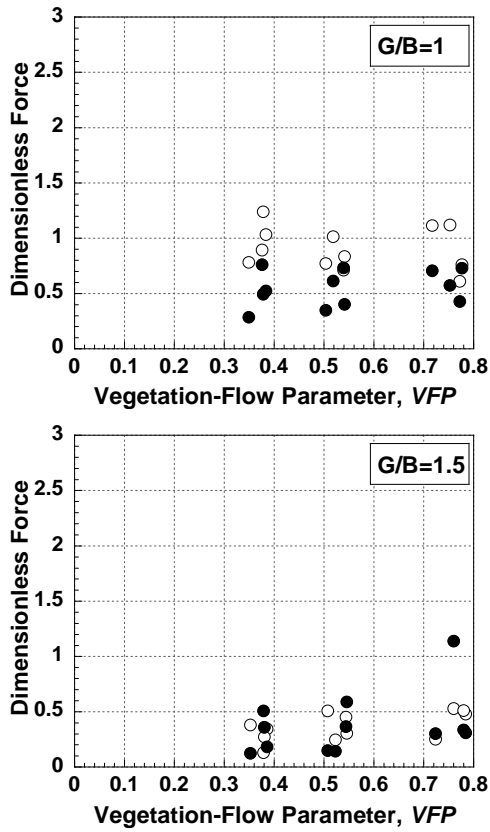


Fig. 15 Variation of Dimensionless Force with Vegetation-Flow Parameter for  $(BG*SP/D^2) = 750$ . (○-No Veg and ●-Veg)

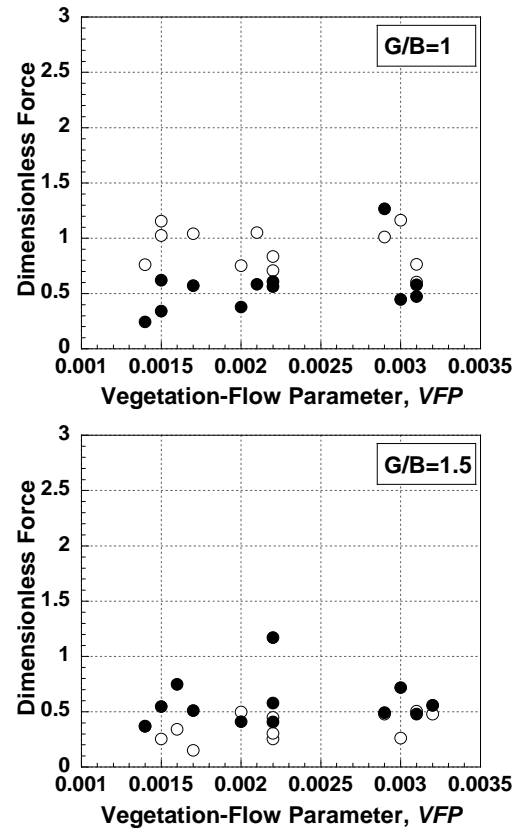
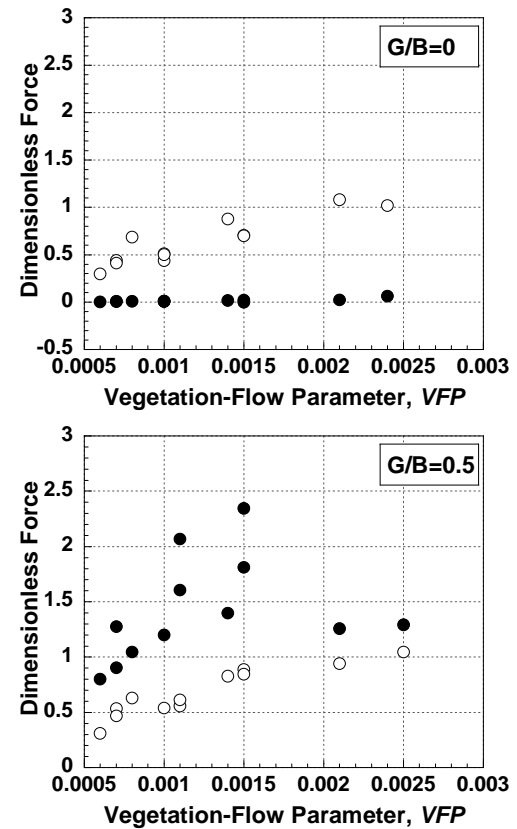
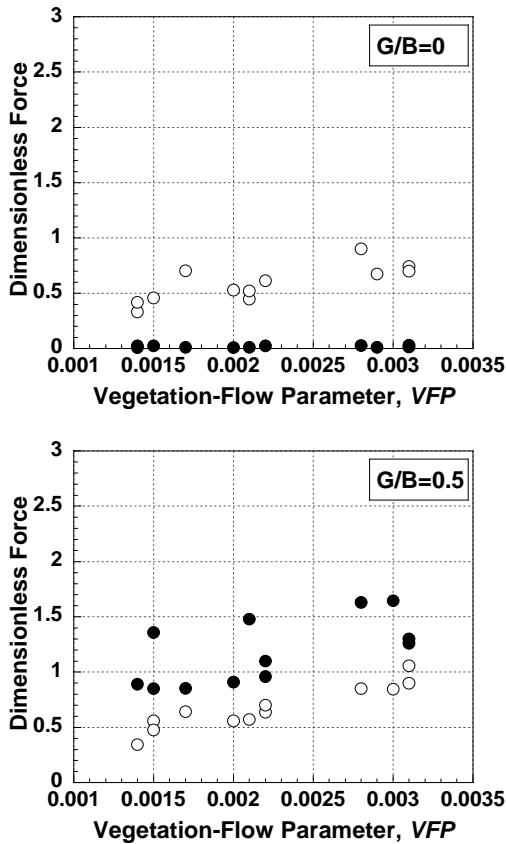


Fig. 16 Variation of Dimensionless Force with Vegetation-Flow Parameter for  $(BG*SP/D^2) = 1040$ . (○-No Veg and ●-Veg)



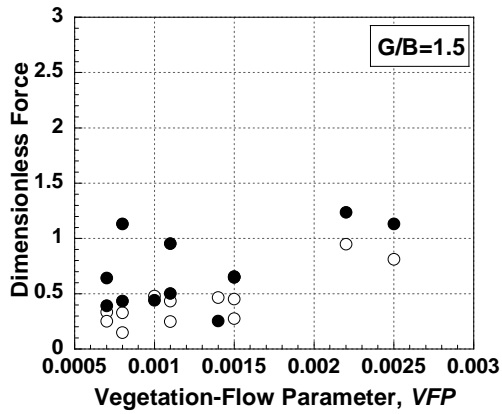
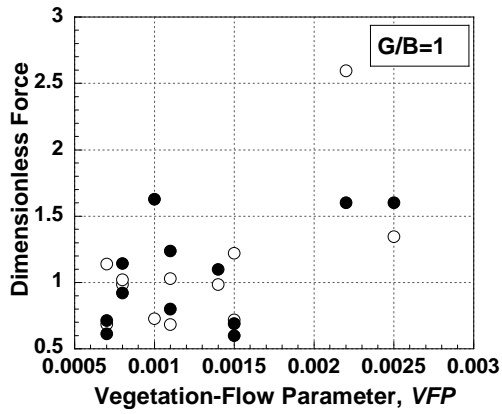


Fig. 17 Variation of Dimensionless Force with Vegetation-Flow Parameter for  $(BG*SP/D^2) = 2080$ . (○-No Veg and ●-Veg)

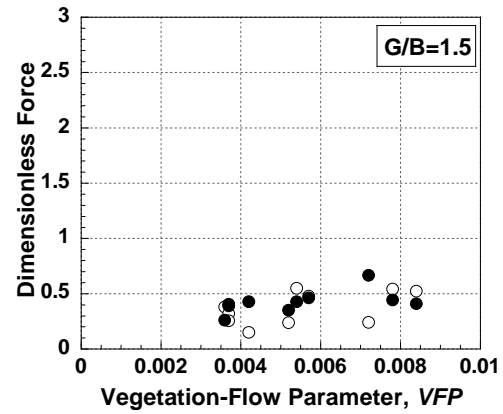
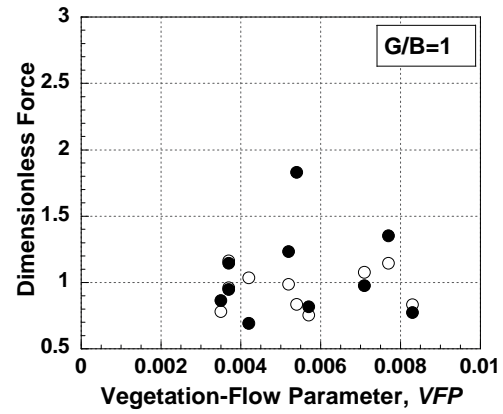
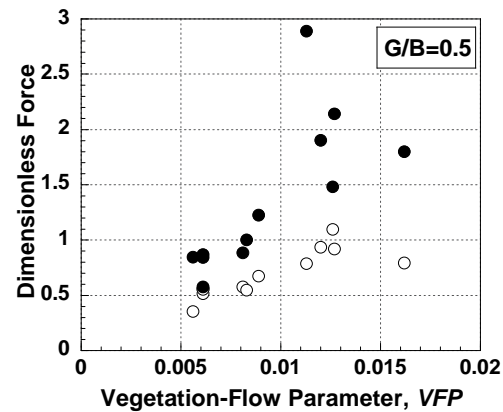
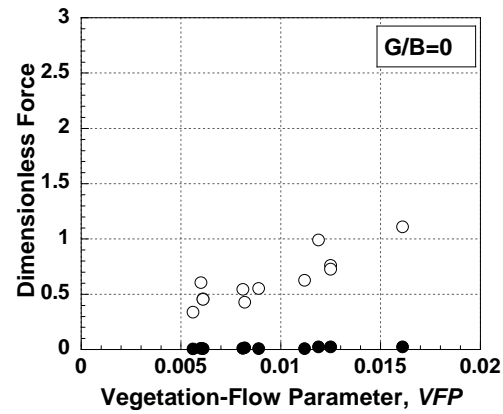
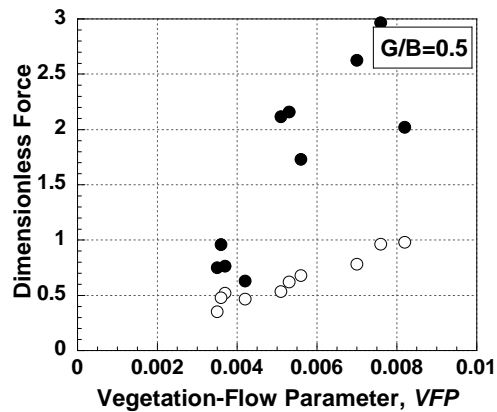
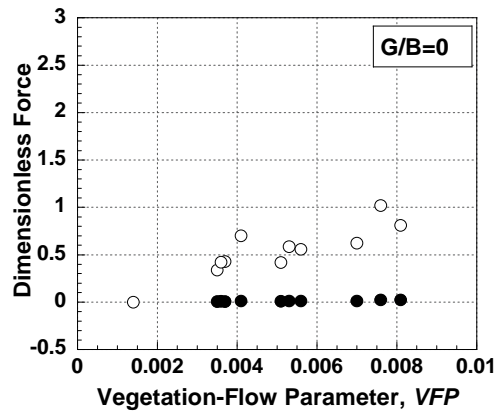


Fig. 18 Variation of Dimensionless Force with Vegetation-Flow Parameter for  $(BG*SP/D^2) = 2604$ . (○-No Veg and ●-Veg)



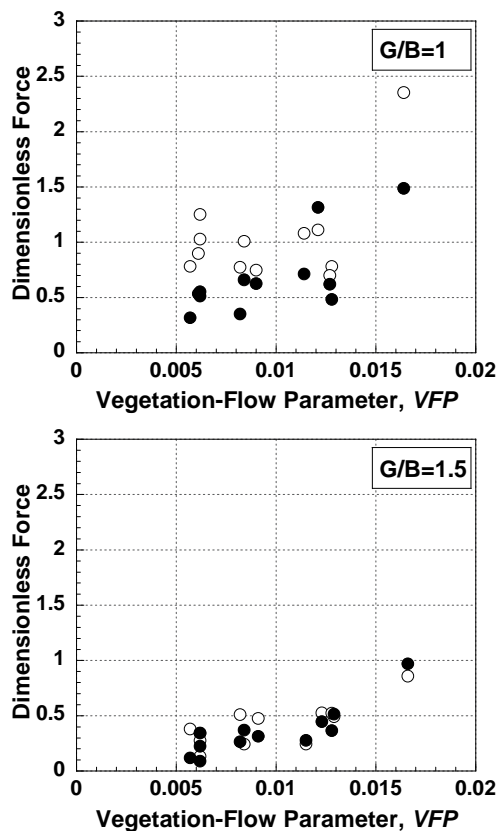


Fig. 19 Variation of Dimensionless Force with Vegetation-Flow Parameter for  $(BG*SP/D2) = 4166$ . (○-No Veg and ●-Veg)

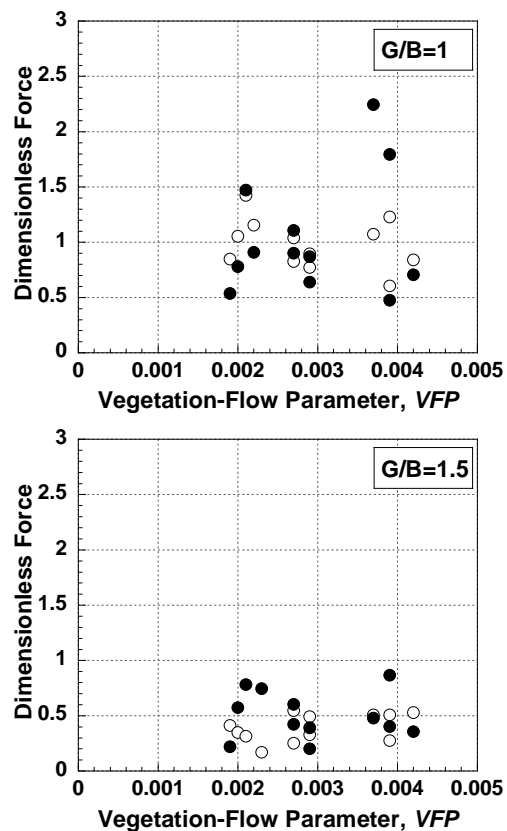
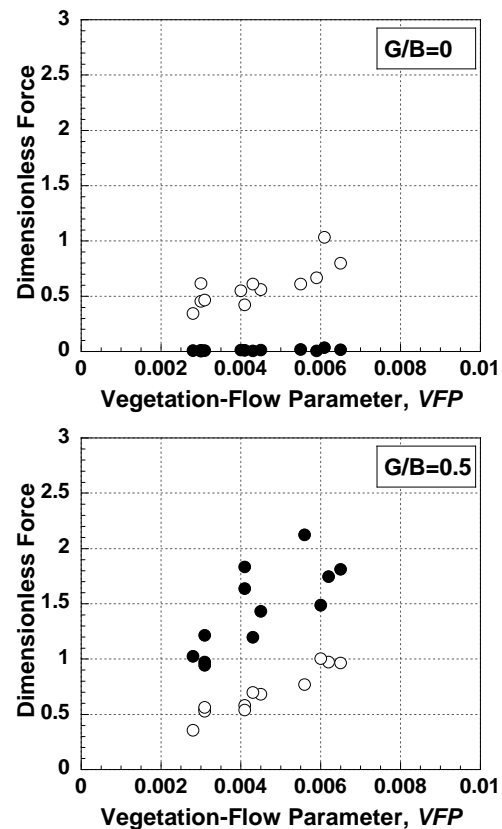
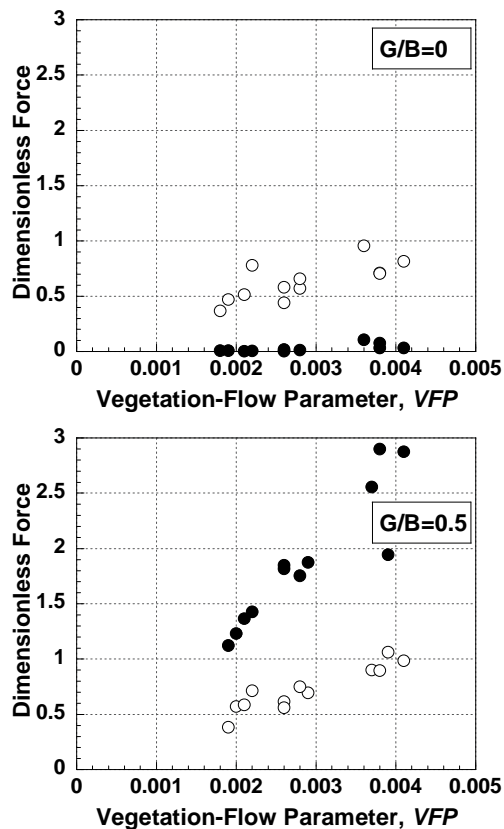


Fig. 20 Variation of Dimensionless Force with Vegetation-Flow Parameter for  $(BG*SP/D2) = 5208$ . (○-No Veg and ●-Veg)



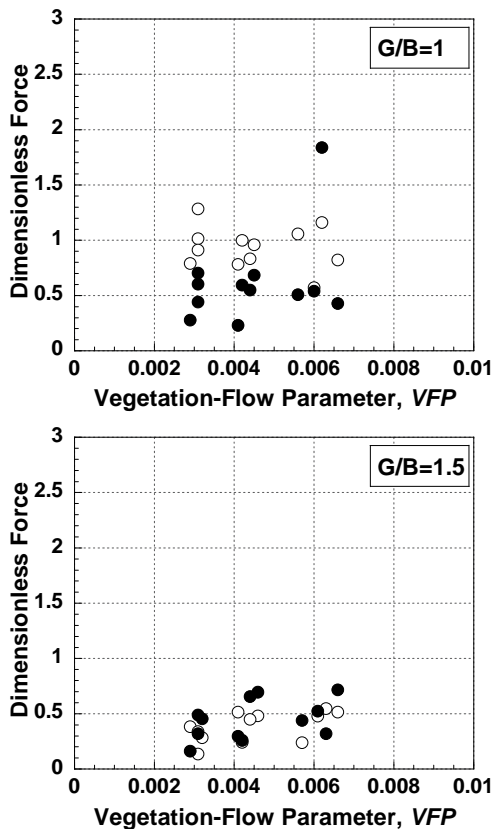


Fig. 21 Variation of Dimensionless Force with Vegetation-Flow

Parameter for  $(BG*SP/D2) = 8333$ . (○-No Veg and ●-Veg)

It is also observed that the  $F^*$  has a linear relationship with VFP for a given  $[BG*SP/D2]$ . Further, most of the results pertaining to  $G/B = 1.5$  show that the forces are mostly lower, in case of a building fronted by vegetation compared to that with no vegetation. Hence it may be concluded that if  $G/B$  is greater than 1.5, the reduction of forces on a building fronted by vegetation will be more effective.

There are two main types by which the vegetation can be classified, as densely placed and sparsely placed. Vegetation of larger diameter and smaller spacing refers to densely placed and the smaller diameter and larger spacing refers to sparsely placed vegetation. Based on the above discussions, by inter-comparison of Figs. 10 to 21, it may be stated that sparsely placed vegetation has a certain advantage as the vegetal drag is present and also no appreciable increase in kinetic energy on the lee side take place, since the cross section of the flow is not reduced much. However, in the case of densely placed vegetation, there could be more drag and a possibility of appreciable increase in the kinetic energy due to reduction in area of cross section of flow area. Hence, the optimum configuration may be obtained using the VFP and  $[BG*SP/D^2]$ .

The experimental data on  $F^*$  were finally subjected to a percentile analysis in order to have a better understanding on the effect of  $G/B$ . The variation of percentage of occurrence of force,  $F^*$  on the model building/ structure for the two scenarios, viz., (a) structure fronted by vegetal model/ bio shield and (b) structure with no vegetation

present have been plotted in Figs. 22a and 22b respectively. Percentage of occurrence has been used as a measure to have an idea of how many test cases have a lower force magnitude than a value with some specific force magnitude for all the vegetation and flow parameters experimented. The aforementioned has been illustrated by the below mentioned example.

The model building/structure with no vegetation present, the percentages of occurrence of  $F^* \leq .75$  for  $G/B = 0.0, 0.5, 1.0$  and  $1.5$  are found to be about 75%, 59%, 12% and 91% respectively. This depicts that the structure with the absence of the vegetal model, the force  $F^*$  seems to be maximum for  $G/B$  ratio 1.0 and it got reduced for the  $G/B$  ratio of 1.5 too. If this analogy is adopted to the forces on the structures fronted by vegetation for the same reference  $F^* \leq .75$ , the percentile for  $G/B = 0.0, 0.5, 1.0$  and  $1.5$  is 100%, 5%, 55% and 81% respectively. As all experiments have been conducted for a very high Ursells number, the desirable distances to be adopted between the vegetal model/ bio shield and the modeled building/ structure would either  $G/B = 0$  or  $G/B > 1.5$ .

#### A. The Role of Vegetation in Reducing the Forces

Among the  $G/B$  ratios experimented, forces found to have a smaller magnitude particularly for the  $G/B = 0$  and  $G/B = 1.5$  as well. This reduction in the  $F^*$  is owing to the frictional effect that the slope offered by the time the jet of water runs off a sufficient distance from the reference line. During this running off process the water jet also lost some amount of its kinetic energy. On the other hand for the case of  $G/B = 0.5$  and  $G/B = 1$ , running off water past vegetation with more kinetic energy strikes the structure, where  $F^*$  is being measured without losing its energy as it runs off only a shorter distance on the slope and hence the slope even would not offer any kind of frictional resistance as in the case of  $G/B = 0$  and  $G/B = 1.5$ . Also the run up height seemed to be approximately  $2H$ , for  $G/B = 0$  and  $1.5$ . Water particles past the vegetation with more kinetic energy gets amplified at the exit of the vegetal patch because of the resistance that has been offered by the vegetal model/ bio shields. In addition to the above mentioned amplification of energy in the water particles, splashing of water particles also plays a vital role in aggravating the magnitude of the forces on the model building/structures. So in a nutshell, the amplification of the water particles combined with splashing has been the cause for the increment in forces,  $F^*$  on the model building and hence for the  $G/B$  ratios of 0.5 and 1.0 exerts higher degree of magnitude forces when it is compared with the other  $G/B$  ratios of 0 and 1.5. As the splashing water particles impinge on the structure, forces get magnified for the cases of  $G/B$  ratios 0.5 and 1.0. It is to be noted that the splashing and impingement does not occur for the  $G/B$  ratio of 0 and hence a greater force reduction has been observed.

The results from the present work can help the planners in planning and designing the bio-shield. The most important parameters of the bio-shields such as its width, the diameter of the individual stems, the spacing between them as well as the distance between the bio-shield and the structure which is to be protected can be ascertained.

## V. SUMMARY AND CONCLUSION

The variation of forces on a structure placed at  $G/B = 0, 0.5, 1.0$  and  $1.5$  from the green belt/ bio shield which is subjected to large Ursell number (Cnoidal waves) has been presented in detail in this paper. The forces that the structure experienced for various Vegetation Flow Parameter and Vegetal Parameter have been studied and presented. The  $[BG*SP/D^2]$ , Vegetal Parameter helps in understanding the behavior of the vegetation and its location from the reference line. The forces,  $F^*$  measured for the case with vegetation for  $G/B = 0$  and  $G/B > 1.5$  has reduced the  $F^*$  to a greater degree of extent when it is compared with the case where there is no vegetation present. On the other hand  $G/B = 0.5$  has increased the  $F^*$  and thus caused a reverse effect.

Using the formulae of the present work, duly knowing the environmental features/conditions of a particular location, where the bio-shield could be proposed as a buffer system for effectively attenuating the extreme wave forces  $F^*$ , one can choose the type of vegetation to be planted that would survive. A number of species are available with a wide range of properties with different number of years for its fully grown characteristics. These could serve us, as guidelines for proper planning that would depend on the nature of mitigation measure, that is, long or short term. The

present work helps to arrive at the parameters of the Bio-shield such as  $BG, SP$  and  $D$  in the design of bio-shield in order to ensure that its presence would not allow the wave force on the structure on its leeside to exceed a certain value, that is, the design force of the structure under consideration. Hence with the help of the empirical equations and the characteristics of the species, one can match the bio-shield parameters to suit the wave and environmental conditions of the location.

## A. How to Apply the Results of the Experiments?

In the present study the rigidity of the vegetation has been modeled,  $EI$ . This work is not case/ site specific. For an example, if a particular location/ coast needs to be protected by Bio-shield against a 3m wave in the sense, then we can easily calculate the hydrodynamic waves forces,  $F^*$  from the Equation 1. The force is expressed in a dimensionless form as Equation 1. Then we can find the value of  $VFP$ , from the plots (Fig. 9 to Fig. 22) for a particular value of  $G/B$ . By suitably substituting the values for the variables ( $BG, SP$  and  $D$ ) in the  $VFP$  we can arrive at the design parameters of the Bio-shield/ Green belt. It is possible to obtain the optimum configuration using the  $VFP$  and  $[BG*SP/D^2]$ . Fig. 23, exhibits the schematic representation of the aforesaid facts.

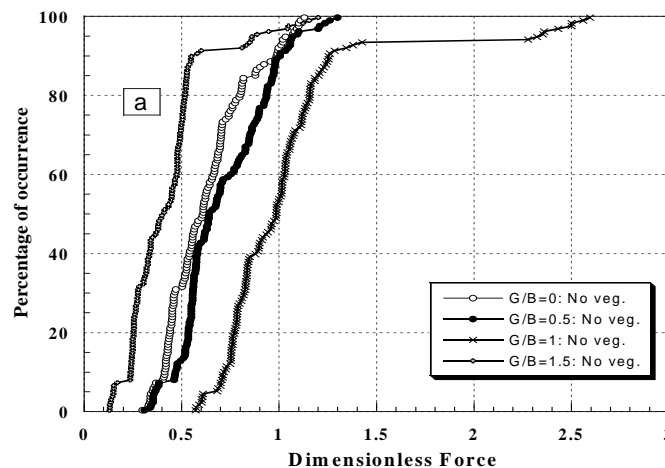


Fig. 22a Percentage of occurrence of force in the absence of vegetation

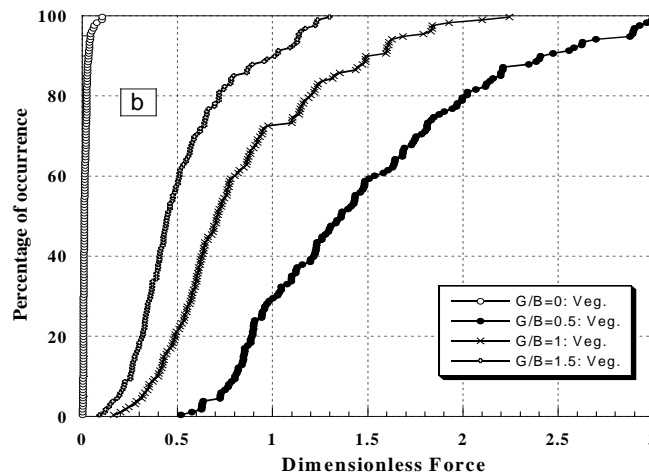


Fig. 22b Percentage of occurrence of force in the presence of vegetation



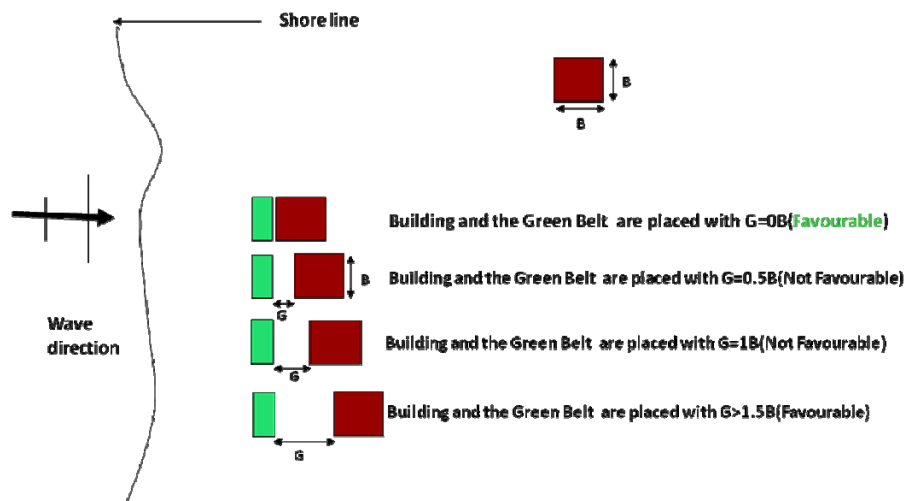


Fig. 23 Schematic representation of the Bio shield and the model building/ structure

#### REFERENCES

- [1] Borrero, J. C., Sieh, K., Chlieh, M., Synolaki, C.E., 2006. Tsunami inundation modeling for western Sumatra. *Proc. Natl Acad Sci.* 103(52): 19673-196.
- [2] Chakrabarti, S.K., 1983. *Hydrodynamics of offshore structures.* Computational Mechanics Publications, Southampton Boston.
- [3] Danielsen, F., Sørensen, M.K., Olwig, M.F., Selvam, V., FaizalParish, Neil, D., Burgess, Hiraishi, T., Karunakaran, V.M., Rasmussen, M.S., Hansen, L.B., Quarto, A., Suryadiputra. N., 2005. A Protective Role for Coastal Vegetation. *Science, New Series*, Vol. 310, No. 5748, 643.
- [4] Gan, K.S., Lim, S.C., Choo, K.T., Jantan, M.D., 2001. Timber notes-medium hardwoods 4. *Timber Technology Bulletin* 21, 1-7.
- [5] Harada, K., Imamura, F., 2005. Effects of coastal forest on tsunami hazard mitigation – A preliminary investigation. *Tsunamis, Case Studies and Recent Developments*, Springer, Netherlands, 279-292.
- [6] Hiraishi, T., Harada, K., 2003. Greenbelt Tsunami Prevention in South Pacific region, Report of the port and airport research institute, Vol.42. No.2.
- [7] Hiraishi, T., 2005. Greenbelt technique for tsunami disaster reduction. *APEC-EqTAP Seminar on Earthquake and Tsunami Disaster Reduction Jakarta, Indonesia*, 1-6.
- [8] Issacson, M., de St. Q., 1979. Wave Force On Large Square Cylinders. In *mechanics of wave-induced force on cylinders*, ed. T. L. shaw, Pitman, London, 609-622.
- [9] Kathiresan, K., Rajendran N., 2005. Coastal mangrove forests mitigated tsunami. *Estuarine, Coastal and Shelf Science* 65 (3), 601-606.
- [10] Kongko, W., 2005. Mangrove as a Tsunami Reduction and its Application. *APEC-EqTAP Seminar on Earthquake and Tsunami Disaster Reduction, Jakarta, Indonesia*.
- [11] Laso-Bayas, J. C. C. Marohn., G. Dercon, S. Dewi, H. P. Piepho, L. Joshi, M. van Noordwijk, & G. Cadisch. 2011. Influence of coastal vegetation on the 2004 tsunami wave impact in west Aceh. *Proc. Natl Acad Sci.* 108(46): 18612-18617.
- [12] Nandasena, K.N.A., Tanaka, N., 2007. Elucidating effectiveness of dominant types of coastal vegetation found in Sri Lanka for tsunami protection in numerical modeling. *Annual Research Journal of SLSAJ*, 6, 16-21.
- [13] Noarayanan, L., Murali, K. and Sundar, V., 2011. Role of vegetal configuration on the pressures due to cnoidal waves on a wall. *The International Journal of Ocean and Climate Systems*, 2 (3), 169- 188.
- [14] Noarayanan, L., Murali, K. and Sundar, V., 2012. Attenuation of Run-up due to regular and cnoidal waves by seaward vegetation. *Journal of coastal research*, 28 (1A), 123-130.
- [15] Noarayanan, L., Murali, K. and Sundar, V., 2012, Manning's n co-efficient for flexible emergent vegetation in tandem configuration. *Jl of Hydro Environment research (JHER)*, 6, 51-62.
- [16] Struve, J., Falconer, R.A., Wu, Y., 2003. Influence of model mangrove trees on the hydrodynamics in a flume. *Estuarine, Coastal and Shelf Science* 58 (1), 163-171.
- [17] Sundar, V., Sannasiraj, S.A., Murali, K., Sundaravadeivelu, R., 2007. Run-up an inundation along the Indian Peninsula including Andaman Islands due to great Indian ocean tsunami. *Journal of waterway, port, coastal, and ocean engineering*, ASCE, 133 (6), 401-413.
- [18] Tanaka, N., Sasaki, Y., Mowjood M.I.M., Jinadasa, K.B.S.N., Homchuen S., 2007. Coastal vegetation structures and their functions in tsunami protection: experience of the recent Indian Ocean tsunami. *Landscape and Ecological Engineering* 3 (1), 33-45.
- [19] Wiegel, R.L., 1964. *Oceanographical Engineering*, Published by Prentice-hall, INC/Englewood cliffs, N.J., USA.

#### Notation

The following symbols are used in this paper:

|       |   |   |
|-------|---|---|
| $B_s$ | = | Width of the structure;                 |
| $BG$  | = | Width of green belt;                    |
| $D$   | = | Diameter of vegetal stem;               |
| $D_b$ | = | Diameter at the root of the vegetation; |
| $D_s$ | = | Width of the structure;                 |



|           |   |  |
|-----------|---|--|
| $E$       | = | Modulus of elasticity;                       |
| $f_1$     | = | Frequency of first mode of the vegetal stem; |
| $F_{max}$ | = | Maximum measured force;                      |
| $F^*$     | = | Dimensionless force;                         |
| $g$       | = | Gravitational constant;                      |
| $h$       | = | Depth of flow;                               |
| $h_s$     | = | Depth of water at the toe of the structure;  |
| $H$       | = | Wave height;                                 |
| $I$       | = | Second moment of inertia;                    |
| $L$       | = | Wave length;                                 |
| $l$       | = | Height of the vegetation;                    |
| $R_u$     | = | Run-up;                                      |
| $KC$      | = | Keulegan–Carpenter number;                   |
| $SP$      | = | Spacing of the vegetation;                   |
| $T$       | = | Time period;                                 |
| $U_{max}$ | = | Maximum orbital velocity under waves;        |
| $V$       | = | Flow velocity;                               |
| $V_{avg}$ | = | Average velocity;                            |
| $V_r$     | = | Reduced velocity;                            |
| $VFP$     | = | Vegetation Flow Parameter; and               |
| $\beta$   | = | Beach slope;                                 |
| $\rho$    | = | Mass density of water;                       |

### Appendix-A.

#### Design Procedure of a Bio Shield

|   |     |
|---|-----|
| $F^* = [(F_{max}) / (0.5\rho g H^2 B_s)]$               | A-1 |
| $VFP = [EI (BG/D) / (\rho H^3 V_{avg}^2 (SP/D))]$       | A-2 |
| Keulegan–Carpenter, $KC$ number = $(U_{max} * T) / D_s$ | A-3 |
| Reduced Velocity, $V_r = [V_{avg} / (f_1 D)]$           | A-4 |
| Vegetation Parameter is $[BG * SP / D^2]$ .             | A-5 |

Keulegan–Carpenter number, is a dimensionless quantity that which describes the relative importance of the drag forces over inertia forces for any objects in an oscillatory fluid flow and is expressed as  $U_{max} * T / D$ . Where,  $U_{max}$  is approximated as  $[c = \sqrt{gh_s(1+(H/h_s))}]$ ;

### Design procedure of bio-shield

1. In the first step the designer should have to have an approximate force magnitude that the structure on the lee side of the proposed plantation can withstand.
2. The  $G/B$  ratio to be adopted can be obtained from the maximum force as per the requirement cited under Item 1.
3. Choose the type of vegetation that can grow in the site for implementation.
4. Once the type of vegetation is chosen then the strength characteristics of the individual tree within the greenbelt can be ascertained.

5. Now assuming a value for  $BG$ , find vegetation parameter,  $VFP$ .
6. Then by substituting the wave and flow parameters in A-2 one can determine the  $VFP$ .
7. From Steps 5 and 6 we know which of the plots can be used for calculating maximum force and cross check.
8. By changing the variables in A-5, the above mentioned Steps 6 and 7 are to be repeated until the approximate force magnitude on the lee side of the proposed plantation is achieved.



**Noarayanan Lakshmanan** was born in sirukudalpatti, tamilnadu, INDIA on June 02, 1973. He completed his bachelor degree in Civil Engineering in 1995 and Master of Engineering in Structural Engineering in 2003 both from Mepco Schlenk Engineering College affiliated to Madurai Kamaraj University. In 2009, he completed his Ph.D from Ocean Engineering Department, IIT Madras. He is presently working as a Research Fellow in Nanyang Technological University, Singapore since 2010. He has 11 publications to his credit.

Doctor Lakshmanan has intensively researched on flow-vegetation interaction and specialises in experimental techniques.



**Murali Kantharaj** was born in Polur, Tamilnadu, INDIA on September 06, 1969. After completing his school, he moved to Kancheepuram for his Bachelor degree in Civil Engineering. He later became a GATE scholar and completed his M.Tech. (Ocean Engineering) and Ph.D. (Marine Hydrodynamics) from IIT Madras, Chennai, INDIA.

During his doctoral research period, he parallelly pursued his career as Project Officer and developed computational tools for nearshore dynamics. Later, after obtaining his doctorate, he moved to National University of Singapore to pursue postdoctoral research in headland bays and their stability. In order to be more effective in application of hydrodynamics models, he started to focus on application of CFD methodologies to marine hydrodynamics including parallel computing, free surface dynamics and multiphase flow computations from Institute for High Performance Computing (IHPC), Singapore from 1999 - 2003. Returning to IIT Madras in 2003 as Assistant Professor, he further developed methodologies for application of CFD to hydrodynamics and earned his Professorship in 2009.

Professor Kantharaj is also a member of IAHR, RINA and ASCE. Presently he is also serving as member of Executive Council of IAHR-APD.



**Vallam Sundar** completed his Bachelor degree in Civil Engineering in University of Madras in 1975 followed by M.Tech (Hydraulics) in 1977 and in 1982 both from. He is presently a Professor in Department of Ocean Engineering. He was Head of the Department from 2003 to 2006. He has 400 publications to his credit and has completed 150 projects related to coastal, ocean engineering and port & harbor engineering. He is a recipient of several prizes and awards that includes honorary doctorate degree from University of Wuppertal, Germany for his contributions in teaching and research in the field of Coastal Engineering. He is a member of professional bodies like IAHR, PIANC, CERF and

ASCE. He has also served as Vice Chairman IAHR-APD during 2005-2006 and later Chairman from 2006-2011. He has organized 3 major international conferences, several short courses and workshops includes honorary doctorate degree from University of Wuppertal, Germany for his contributions in teaching and research in the field of Coastal Engineering.

Professor Sundar is a member of professional bodies like IAHR, PIANC, CERF and ASCE. He has also served as Vice Chairman IAHR-APD during 2005-2006 and later Chairman from 2006-2011. He has organized 3 major international conferences, several short courses and workshops.